

Micro pencil with cesium atoms

S.-B. BALMUS*, D. D. SANDU^a

Science Department, "Al. I. Cuza" University of IASI, Romania

^aFaculty of Physics, "Al. I. Cuza" University of IASI, Romania

Manipulation of atoms with laser fields is a very important physical process in controlling atom flux for direct "nano" and "micro" writing on surfaces, making photosensitive nanophotocathode arrays on semiconductors and guiding atoms through surface-plasmon and resonant-ring structures.

(Received April 22, 2010; accepted July 14, 2010)

Keywords: Atom manipulation, Scattered laser fields, Metallic micro thin film, Cs two-level atom model

1. Introduction

The laser field scattered by a special metallic micro thin film acts on Cs atom trajectories in the near field region. This effect makes possible the manipulation of Cs atoms to obtain a micropencil for writing on surfaces and some other applications (realization of periodical Cs atoms array on semiconductors). In this paper we present the most important relations regarding the interaction of electromagnetic laser fields with the Cs "two-level atom" based on Schrödinger equation. Also, some results concerning the possibility and the conditions to use these fields for Cs atoms manipulation are discussed.

2. The two-level model of Cs atom

For characterizing the interaction between a Cs atom and an electromagnetic laser field with a frequency ω closed to Cs s-p transition, the two-level model of the Cs atom, using the electronic basis functions $|s,0\rangle, |p,-1\rangle, |p,0\rangle, |p,1\rangle$, is presented in Fig. 1. [1]

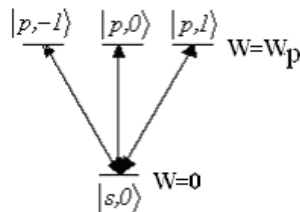


Fig. 1. The two-level Cs atom model.

The Schrödinger equation for electrons has the form [2], [3]:

$$i\hbar|\dot{\Psi}\rangle = (H_{el} - \vec{d} \cdot \hat{e}E_0 \cos \omega t)|\Psi\rangle \quad (1)$$

where H_{el} is the electronic Hamiltonian, \vec{d} is the dipole moment of the atom, \hat{e} is the unit vector of the electric

field, E_0 is the electric field amplitude and ω the pulsation of the electromagnetic laser field.

The wave function $|\Psi\rangle$ and its derivative $|\dot{\Psi}\rangle$ have the expressions:

$$\begin{aligned} |\Psi\rangle &= c_0|s,0\rangle + c_1|p,-1\rangle + c_2|p,0\rangle + c_3|p,1\rangle \\ |\dot{\Psi}\rangle &= \dot{c}_0|s,0\rangle + \dot{c}_1|p,-1\rangle + \dot{c}_2|p,0\rangle + \dot{c}_3|p,1\rangle \end{aligned} \quad (2)$$

where c_0, c_1, c_2, c_3 are the electronic basis function's coefficients and $\dot{c}_0, \dot{c}_1, \dot{c}_2, \dot{c}_3$ represent their derivatives.

Equation (1) can be expressed using the electronic basis functions as follows [3,4]

$$i\hbar \begin{bmatrix} \dot{c}_0 \\ \dot{c}_1 \\ \dot{c}_2 \\ \dot{c}_3 \end{bmatrix} = [A] \begin{bmatrix} c_0 \\ c_1 \\ c_2 \\ c_3 \end{bmatrix} \quad (3)$$

Or

$$i\hbar \begin{bmatrix} \dot{c}_0 \\ \dot{c}_1 \\ \dot{c}_2 \\ \dot{c}_3 \end{bmatrix} = \begin{bmatrix} 0 & M_{01} \cos \omega t & M_{02} \cos \omega t & M_{03} \cos \omega t \\ M_{10} \cos \omega t & E_p & 0 & 0 \\ M_{20} \cos \omega t & 0 & E_p & 0 \\ M_{30} \cos \omega t & 0 & 0 & E_p \end{bmatrix} \begin{bmatrix} c_0 \\ c_1 \\ c_2 \\ c_3 \end{bmatrix} \quad (4)$$

where the following notations are used:

$$\begin{aligned} M_{01} &= -\langle s,0|\vec{d} \cdot \hat{e}|p,-1\rangle E_0 \\ M_{02} &= -\langle s,0|\vec{d} \cdot \hat{e}|p,0\rangle E_0 \\ M_{03} &= -\langle s,0|\vec{d} \cdot \hat{e}|p,1\rangle E_0 \\ M_{10} &= -\langle p,-1|\vec{d} \cdot \hat{e}|s,0\rangle E_0 \\ M_{20} &= -\langle p,0|\vec{d} \cdot \hat{e}|s,0\rangle E_0 \\ M_{30} &= -\langle p,1|\vec{d} \cdot \hat{e}|s,0\rangle E_0 \end{aligned} \quad (5)$$

Using the transformations of variables:

$$\begin{aligned}
d_0 &= c_0 & \dot{d}_0 &= \dot{c}_0 \\
d_1 &= e^{i\omega t} c_1 & \dot{d}_1 &= i\omega e^{i\omega t} c_1 + e^{i\omega t} \dot{c}_1 \\
d_2 &= e^{i\omega t} c_2 & \dot{d}_2 &= i\omega e^{i\omega t} c_2 + e^{i\omega t} \dot{c}_2 \\
d_3 &= e^{i\omega t} c_3 & \dot{d}_3 &= i\omega e^{i\omega t} c_3 + e^{i\omega t} \dot{c}_3
\end{aligned} \quad (6)$$

Schrödinger equation becomes

$$\begin{aligned}
i\hbar\dot{d}_0 &= i\hbar\dot{c}_0 = M_{01} \cos \omega t c_1 + M_{02} \cos \omega t c_2 + \\
&+ M_{03} \cos \omega t c_3 = M_{01} \cos \omega t e^{-i\omega t} d_1 + \\
&+ M_{02} \cos \omega t e^{-i\omega t} d_2 + M_{03} \cos \omega t e^{-i\omega t} d_3 \\
i\hbar\dot{d}_1 &= -\hbar\omega d_1 + e^{i\omega t} M_{10} \cos \omega t c_0 + e^{i\omega t} E_p c_1 \\
&= (E_p - \hbar\omega) d_1 + M_{10} \cos \omega t e^{i\omega t} d_0 \quad (7) \\
i\hbar\dot{d}_2 &= -\hbar\omega d_2 + e^{i\omega t} M_{20} \cos \omega t c_0 + e^{i\omega t} E_p c_2 \\
&= (E_p - \hbar\omega) d_2 + M_{20} \cos \omega t e^{i\omega t} d_0 \\
i\hbar\dot{d}_3 &= -\hbar\omega d_3 + e^{i\omega t} M_{30} \cos \omega t c_0 + e^{i\omega t} E_p c_3 \\
&= (E_p - \hbar\omega) d_3 + M_{30} \cos \omega t e^{i\omega t} d_0
\end{aligned}$$

In the “rotating wave approximation” RWA [3] we can write

$$\begin{aligned}
e^{-i\omega t} \cos \omega t &= \frac{1}{2} (1 + e^{-2i\omega t}) \approx \frac{1}{2} \\
e^{i\omega t} \cos \omega t &= \frac{1}{2} (1 + e^{2i\omega t}) \approx \frac{1}{2}
\end{aligned} \quad (8)$$

Schrödinger equation takes the form:

$$i\hbar \begin{bmatrix} \dot{d}_0 \\ \dot{d}_1 \\ \dot{d}_2 \\ \dot{d}_3 \end{bmatrix} = \begin{bmatrix} 0 & \frac{1}{2} M_{01} & \frac{1}{2} M_{02} & \frac{1}{2} M_{03} \\ \frac{1}{2} M_{10} & -\Delta & 0 & 0 \\ \frac{1}{2} M_{20} & 0 & -\Delta & 0 \\ \frac{1}{2} M_{30} & 0 & 0 & -\Delta \end{bmatrix} \begin{bmatrix} d_0 \\ d_1 \\ d_2 \\ d_3 \end{bmatrix} \quad (9)$$

where $\Delta = (\hbar\omega - W_p) = \hbar\delta$ is the detuning between the laser frequency and the Cs atom s-p transition frequency.

For weak field and large detuning, we have $\dot{d}_1 \approx 0$, $\dot{d}_2 \approx 0$, $\dot{d}_3 \approx 0$ and Schrödinger equation is

$$\begin{cases} i\hbar\dot{d}_0 = \frac{1}{2} M_{01} d_1 + \frac{1}{2} M_{02} d_2 + \frac{1}{2} M_{03} d_3 \\ 0 = \frac{1}{2} M_{10} d_0 - \Delta d_1 \rightarrow d_1 = \frac{M_{10}}{2\Delta} d_0 \\ 0 = \frac{1}{2} M_{20} d_0 - \Delta d_2 \rightarrow d_2 = \frac{M_{20}}{2\Delta} d_0 \\ 0 = \frac{1}{2} M_{30} d_0 - \Delta d_3 \rightarrow d_3 = \frac{M_{30}}{2\Delta} d_0 \end{cases} \quad (10)$$

Including the last three equations of the system (10) in the first one, we obtain the “one-level-atom” model [3], [4]

$$i\hbar\dot{d}_0 = \frac{1}{4\Delta} (M_{01} M_{10} + M_{02} M_{20} + M_{03} M_{30}) d_0 \quad (11)$$

or

$$i\hbar\dot{d}_0 = U_{eff} d_0 \quad (12)$$

where U_{eff} is the effective potential energy which characterizes the laser field and atom interaction:

$$\begin{aligned}
U_{eff} &= \frac{E_0^2}{4\Delta} [\langle s,0 | \vec{d} \cdot \vec{e} | p,-1 \rangle \langle p,-1 | \vec{d} \cdot \vec{e} | s,0 \rangle + \\
&+ \langle s,0 | \vec{d} \cdot \vec{e} | p,0 \rangle \langle p,0 | \vec{d} \cdot \vec{e} | s,0 \rangle + \langle s,0 | \vec{d} \cdot \vec{e} | p,1 \rangle \langle p,1 | \vec{d} \cdot \vec{e} | s,0 \rangle]
\end{aligned} \quad (13)$$

Next we will calculate the matrix

elements $\langle s,0 | \vec{d} \cdot \vec{e} | p,0,\pm 1 \rangle$. The scalar product $\vec{d} \cdot \vec{e}$ is:

$$\vec{d} \cdot \vec{e} = \sum_{p,q} (-1)^p E_{-p} d_q \quad (14)$$

The electronic wave functions, using spherical electronic basis function $Y_{l,q}(\theta, \phi)$, are [3]:

$$\begin{aligned}
\langle r | s,0 \rangle &= R_s(r) Y_{0,0}(\theta, \phi) \\
\langle r | p,-1 \rangle &= R_p(r) Y_{1,0}(\theta, \phi) \\
\langle r | p,0 \rangle &= R_p(r) Y_{0,0}(\theta, \phi) \\
\langle r | p,1 \rangle &= R_p(r) Y_{1,0}(\theta, \phi)
\end{aligned} \quad (15)$$

Therefore

$$\langle s,0 | \vec{d} \cdot \vec{e} | p,0,\pm 1 \rangle = \sum_{p,q} (-1)^p E_{-p} \langle s,0 | d_q | p,0,\pm 1 \rangle \quad (16)$$

where

$$d_q = -\sqrt{\frac{4\pi}{3}} r Y_{1,q}(\theta, \phi) \quad (17)$$

From equations (15), (16) and (17) we obtain

$$\begin{aligned}
\langle s,0 | d_q | p,m \rangle &= -\sqrt{\frac{4\pi}{3}} e \int_0^\infty r^3 dr R_s^*(r) R_p(r) \cdot \\
&\cdot \left[\int_0^\pi \sin \theta d\theta \int_0^{2\pi} d\phi Y_{0,0}^*(\theta, \phi) Y_{1,q}(\theta, \phi) Y_{1,m}(\theta, \phi) \right] = \\
&= -\sqrt{3} e \int_0^\infty r^3 dr R_s^*(r) R_p(r) \langle 11;00 | 00 \rangle \cdot \langle 11;m,q | 00 \rangle
\end{aligned} \quad (18)$$

Hence:

$$\begin{aligned}
\langle s,0 | \vec{d} \cdot \vec{e} | p,-1 \rangle &= d_{sp} \sum_p (-1)^p E_{-p} \langle s,0 | d_1 | p,-1 \rangle = \\
&= \frac{-d_{sp}}{\sqrt{3}} \sum_p (-1)^p E_{-p} = \frac{-d_{sp}}{\sqrt{3}} \\
\langle s,0 | \vec{d} \cdot \vec{e} | p,0 \rangle &= d_{sp} \sum_p (-1)^p E_{-p} \langle s,0 | d_0 | p,0 \rangle = \\
&= \frac{d_{sp}}{\sqrt{3}} \sum_p (-1)^p E_{-p} = -\frac{d_{sp}}{\sqrt{3}} \\
\langle s,0 | \vec{d} \cdot \vec{e} | p,1 \rangle &= d_{sp} \sum_p (-1)^p E_{-p} \langle s,0 | d_{-1} | p,1 \rangle = \\
&= \frac{-d_{sp}}{\sqrt{3}} \sum_p (-1)^p E_{-p} = \frac{-d_{sp}}{\sqrt{3}}
\end{aligned} \quad (19)$$

and the effective energy of interaction becomes

$$U_{eff} = \frac{E_0^2}{4\Delta} \left[\left| \langle s,0 | \vec{d} \cdot \vec{\varepsilon} | p,-l \rangle \right|^2 + \left| \langle s,0 | \vec{d} \cdot \vec{\varepsilon} | p,0 \rangle \right|^2 + \left| \langle s,0 | \vec{d} \cdot \vec{\varepsilon} | p,l \rangle \right|^2 \right] = \frac{E_0^2 d_{sp}^2}{4\Delta} = \frac{E_0^2 d_{sp}^2}{4\hbar\delta} \quad (20)$$

The motion equations of Cs atoms is governed by the Hamiltonian [5]

$$H = \frac{\vec{p}^2}{2m} + U(\vec{r}) = \frac{\vec{p}^2}{2m} + \frac{E_0^2 d_{sp}^2}{4\hbar\delta}, \quad U(\vec{r}) = \frac{E_0^2 d_{sp}^2}{4\hbar\delta} \quad (21)$$

where

$$\left\{ \begin{array}{l} \dot{x} = \frac{p_x}{m} \\ \dot{y} = \frac{p_y}{m} \\ \dot{z} = \frac{p_z}{m} \\ \dot{p}_x = -\partial U / \partial x \\ \dot{p}_y = -\partial U / \partial y \\ \dot{p}_z = -\partial U / \partial z \end{array} \right. \quad \text{or} \quad \left\{ \begin{array}{l} \dot{x} = v_x \\ \dot{y} = v_y \\ \dot{z} = v_z \\ \dot{v}_x = -\frac{\partial U / \partial x}{m} \\ \dot{v}_y = -\frac{\partial U / \partial y}{m} \\ \dot{v}_z = -\frac{\partial U / \partial z}{m} \end{array} \right. \quad (22)$$

In the case of an electromagnetic laser field scattered by a particular diffraction structure it is convenient to have the potential energy as a function of the ratio between the incident and the scattered electric field. Using the intensity of the laser field we can write for the expression of the potential energy

$$U(\vec{r}) = \frac{d_{sp}^2}{4\hbar\delta} \frac{2I_0}{\varepsilon_0 c} \frac{E^2}{E_0^2} = \frac{d_{sp}^2}{2\hbar\delta} \frac{I_0}{\varepsilon_0 c} \frac{E(\vec{r})^2}{E_0^2} \quad (23)$$

where I_0 (W/m^2) is the intensity of the incident laser field, E_0 is the magnitude of the incident electric field on the scattering micro or nanostructure; $E(\vec{r})$ is the magnitude of the total electric field; $\varepsilon_0 = 8.854 \cdot 10^{-12} F/m$ is the permittivity of free space; $\hbar = 1.054 \cdot 10^{-34} J \cdot s$ is Planck's constant and c is the light speed in free space.

For Cs: $m = 133 a.m.u. = 2.2 \cdot 10^{-25} Kg$ and $d_{sp}^2 = 12.2 \cdot a_0^2 \cdot q^2 = 8.74 \cdot 10^{-58} (C \cdot m)^2$ where:

$a_0 = 0.529 \cdot 10^{-10} m$ is the Bohr-Radius

$q = 1.6 \cdot 10^{-19} C$ is the electronic charge.

* $a.m.u$ – atomic mass unity $1 a.m.u = 1,660 \cdot 10^{-27} Kg$

3. Movement of Cs atoms in the near field of a special metallic micro thin film with a central slit and grooves. Simulation procedures

The micro film presented in Fig. 2. is considered infinite along Oy and its main characteristics are: $a=250nm$ (the width of the central slit and grooves), $d=800nm$ (the period), $h=80nm$ (the depth of the grooves) and $w=300nm$ (the thickness of the metal) in which the corrugation ($M = N = 10$ grooves to the left and right of the

central slit) are placed in the input and in the output surface. The main purpose of the grooves is to focus the scattered field just above the central slit. The output (right) face of the film is characterized by $z=0$.

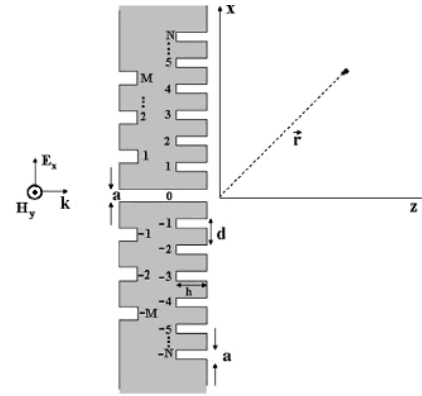


Fig. 2. The metallic film and its dimensions.

The main purpose of the simulations presented below is to verify if it is possible to obtain a micro pencil with Cs atoms using the near field scattered by the thin film for guiding the atoms through the central slit and depositing them on a semiconductor substrate. So, this micro thin film excited by laser field can be used for direct micro writing and for obtaining periodical Cs atoms arrays on semiconductors which have important photosensitive properties and can be used for microelectronic devices. The metallic film is excited from the left side ($z < 0$) with electromagnetic laser plane waves with a wavelength of $852.1 nm$

3.1. Scattered field's structure

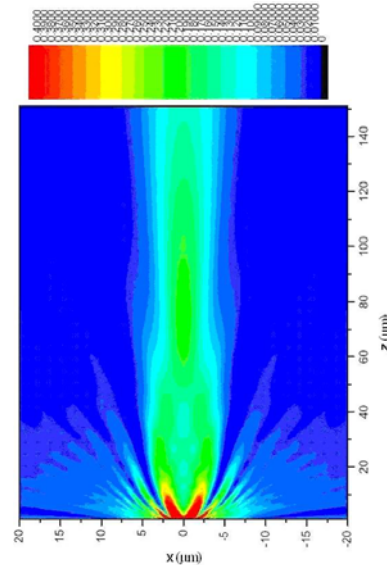


Fig. 3. Relative electric field.

Using the momentum method [6], [8], the relative electromagnetic field structure was calculated above the metallic film ($z > 0$) and it is presented in this section. The

relative field is defined as the ratio between the total (incident and scattered) field and the incident field. The electric field structure calculated above the metallic micro thin film is presented in Fig. 3.

Bellow, in the Figs. 4,5,6,7,8,9,10,11, is presented the relative electric field structure in cross sections for different distances from the film [10,11,12].

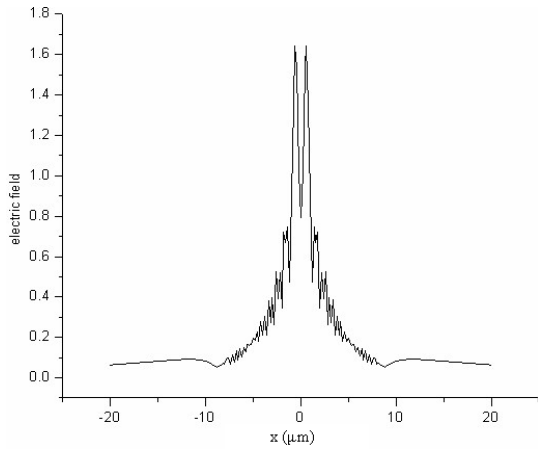


Fig. 4. Relative electric field in cross section at $z = 1 \mu\text{m}$

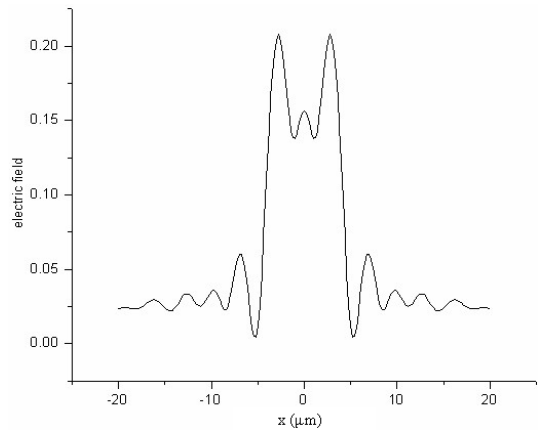


Fig. 5. Relative electric field in cross section at $z = 25.5 \mu\text{m}$

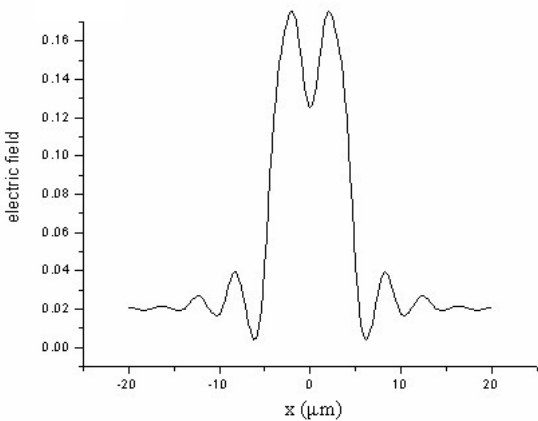


Fig. 6. Relative electric field in cross section at $z = 35.5 \mu\text{m}$

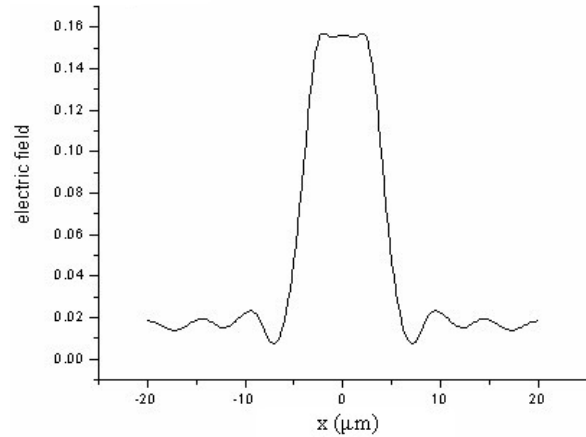


Fig. 7. Relative electric field in cross section at $z = 48 \mu\text{m}$

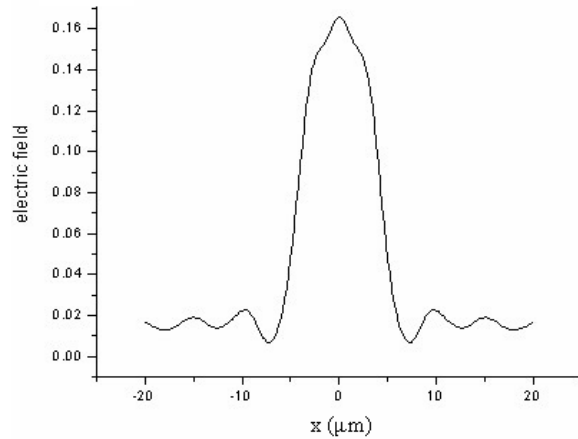


Fig. 8. Relative electric field in cross section at $z = 50.5 \mu\text{m}$.

For $z > 130 \mu\text{m}$ the electric field becomes Gaussian:

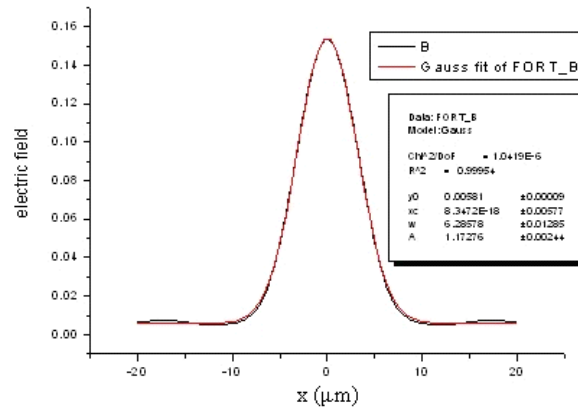


Fig. 9. Relative electric field in cross section at $z = 131 \mu\text{m}$

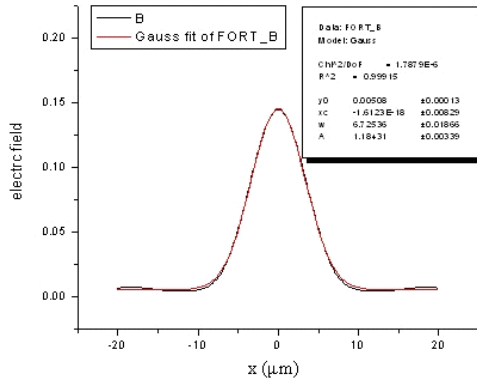


Fig. 10. Relative electric field in cross section at $z = 141 \mu\text{m}$

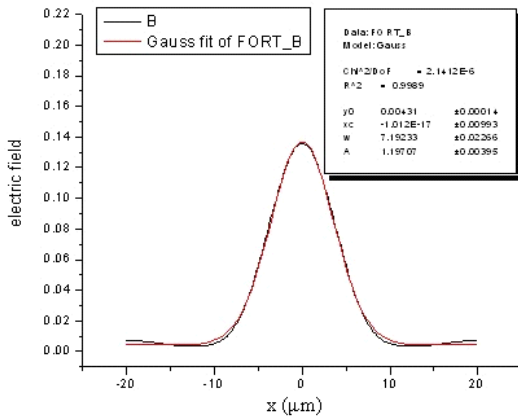


Fig. 11. Relative electric field in cross section at $z = 151 \mu\text{m}$.

3.2. Manipulation of Cs atoms in the described fields. Trajectories

The potential energy (23) is equivalent with

$$U(\vec{r}) = \frac{d_{sp}^2}{2\hbar\delta} \frac{I_0}{\epsilon_0 c} \left(\frac{E(\vec{r})}{E_0} \right)^2 = B \frac{I_0}{\delta} \left(\frac{E(\vec{r})}{E_0} \right)^2 \quad (24)$$

where

$$B = \frac{d_{sp}^2}{2\hbar\epsilon_0 c} \approx 0.156 \cdot 10^{-20} \quad (\text{S.I. unities})$$

$$B = \frac{d_{sp}^2}{2\hbar\epsilon_0 c} \approx 0.0941 \cdot 10^7 \quad (\mu\text{m} \cdot \mu\text{s} \cdot \text{a.m.u.})$$

So, the potential interaction energy becomes

$$U(\vec{r}) = 0.000941 \frac{I_0 (\text{W}/\text{m}^2)}{\delta (\text{GHz})} \left(\frac{E(\vec{r})}{E_0} \right)^2 \quad (25)$$

Depending on the detuning between the laser frequency and Cs s-p transition frequency, to the red (negative) or to the blue (positive), the force which acts between the Cs atoms and the electromagnetic field is attractive or repulsive. Because the relative electric field presents its maximum right above the slit, we will present only the attractive force case (the atoms will migrate there

where the electric field is greater). In the repulsive force case the atoms will migrate in the minimum of the electric field and so they can not be guided through the central slit.

The main purpose of the calculus of the trajectories is to verify if the metallic film and the scattered field could be used for guiding the atoms through the central slit and depositing them on a semiconductor substrate.

For the calculus of the trajectories it is used a Finite Element method [9] with the next steps:

- space division in cubic elements in which the field could be approximate as constant along Ox, Oy and Oz axis. So, the atoms movement can be considered as a Newtonian uniform accelerate movement and because of relative small velocities the relativistic effects are ignored.
- the gravitational and interaction between the Cs atoms forces are ignored; so, only the electromagnetic fields effect can be observed.
- a small time step selection (choice) in order to not exceed the finite element limit in one integration (the spatial step is ten times smaller then the cube size).
- integration of the scalar movement equations.

As a source of Cs atoms it is used a MOT (Magneto Optical Trap) or a Cs atoms oven [7] situated at $z=151 \mu\text{m}$ above the film. In the trajectories calculus it is used a $\delta = 10\text{GHz}$ detuning and an $I_0 = 10^7 \text{W}/\text{m}^2$ incident field intensity. The initial position of Cs atoms is characterized by $z=151 \mu\text{m}$ and randomly x between $-10 \mu\text{m}$ and $10 \mu\text{m}$; the initial velocity of Cs atoms on z is $v_{0z} = -1 \div -10 \mu\text{m}/\mu\text{s}$ and $v_{0x} = 0 \mu\text{m}/\mu\text{s}$. v_{0z} is considered negative because it is orientated in opposite sense with the Oz direction.

3.3 Case of attractive force

Taking into account 100 atoms it were calculated their trajectories, as a function of the initial velocity on Oz direction. Equidistant initial positions were generated ($z_0 = 151 \mu\text{m}$; x_0 between -10nm and 10nm).

These dependences are presented bellow the figures 12, 13, 14, 15, 16, 17

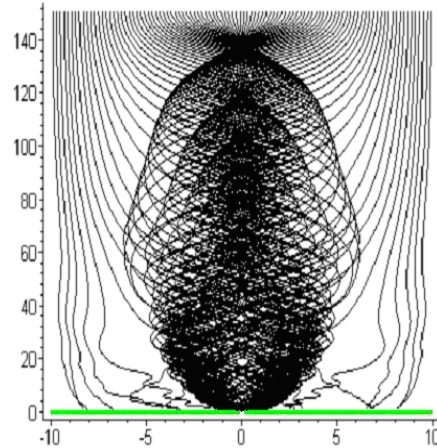


Fig. 12. 100 trajectories for $v_{0z} = -1 \text{ m/s}$

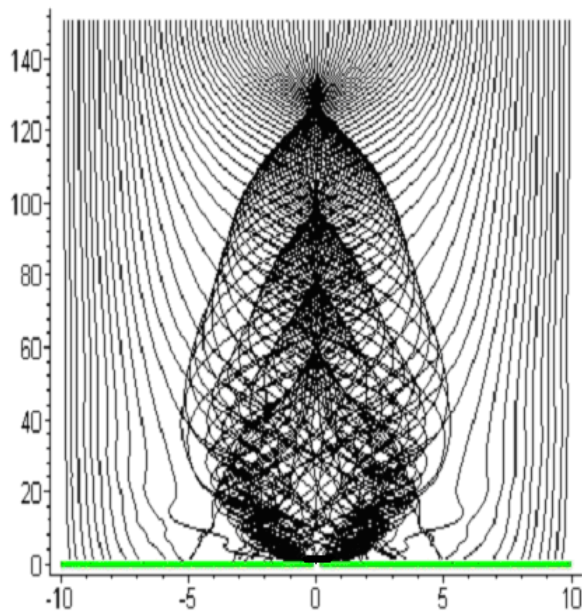


Fig. 13. 100 trajectories for $v_{0z} = -2$ m/s

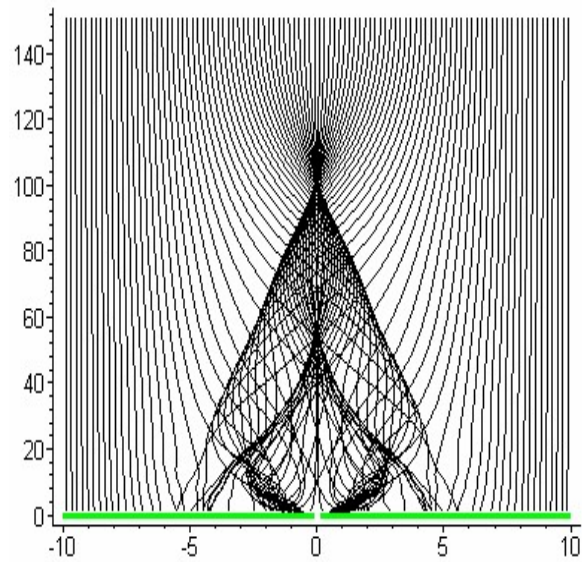


Fig. 14. 100 trajectories for $v_{0z} = -5$ m/s

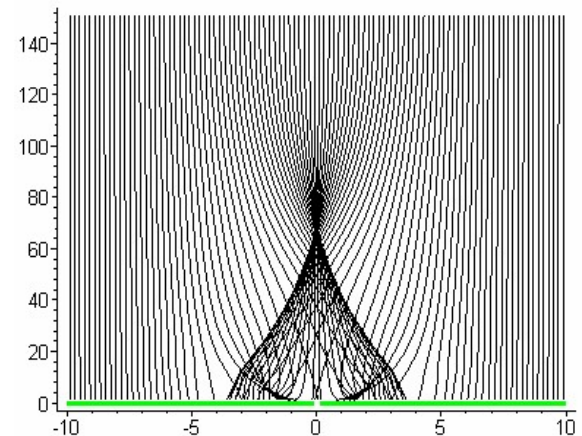


Fig. 15. 100 trajectories for $v_{0z} = -10$ m/s

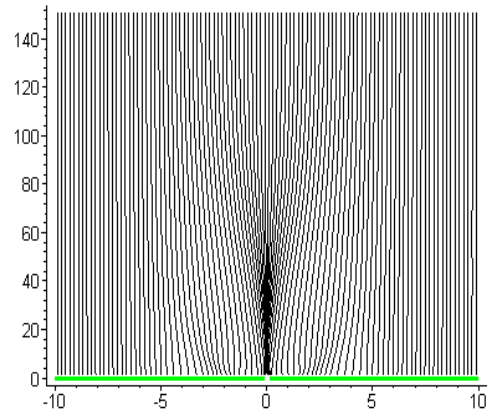


Fig. 16. 100 trajectories for $v_{0z} = -20$ m/s.

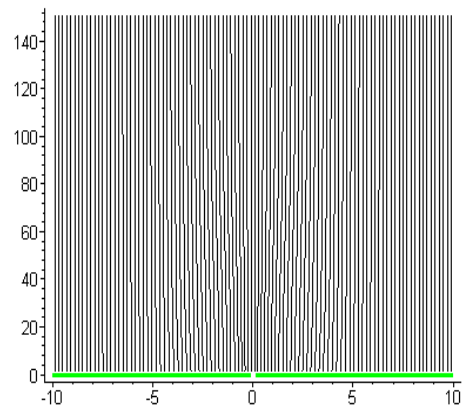


Fig. 17. 100 trajectories for $v_{0z} = -50$ m/s

By adding the gravity forces which act parallel with Oz axis but in the opposite direction and maintaining $v_{0x} = 0 \mu\text{m}/\mu\text{s}$ the next trajectories were obtained (Fig. 18 and 19).

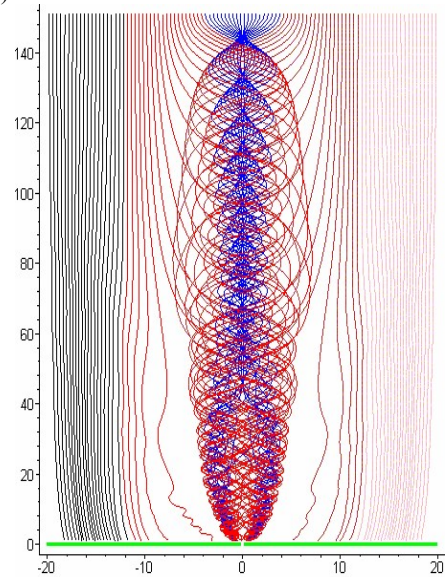


Fig. 18. 100 trajectories for $v_{0z} = -0.5$ m/s, $v_{0x} = 0$ m/s and gravity $g = 10^{-5} \mu\text{m}/\mu\text{s}^2$

We can see from the last simulations that by using this thin film and its near field with its described structure and incident intensity we can manipulate just cold atoms. Practically, we could use as a source of atoms a MOT situated, for technical reasons, at $z > 1 \text{ cm}$ away from the metallic micro film.

In the next simulations we present the trajectories of 100 atoms which arrived in the near field of metallic thin film from a MOT situated at $10 \cdot 10^3 \mu\text{m}$ and characterized by a temperature $T = 50 \mu\text{K}$. Initial velocity on Ox axis $v_{0x} = -1 \div 1 \mu\text{m}/\mu\text{s}$ was also considered.

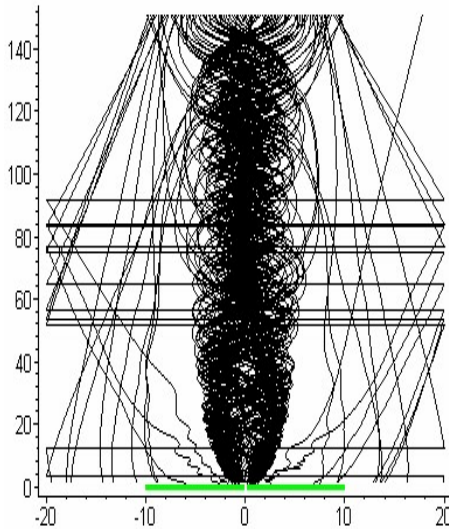


Fig. 19. 100 trajectories for $v_{0z} = -0.5 \text{ m/s}$,
 $v_{0x} = -1 \div 1 \mu\text{m}/\mu\text{s}$ and gravity $g = 10^{-5} \mu\text{m}/\mu\text{s}^2$

4. Conclusions

Using this metallic thin film excited by laser plane waves with an $I_0 = 10^7 \text{ W/m}^2$ incident field intensity, only cold atoms could be guided through the central slit and used for direct micro writing. So, only the atoms provided by a MOT can be manipulated in the described conditions.

The same results can be obtained for greater initial atoms velocities by using more powerful lasers (by increasing the intensity of the incident electromagnetic field).

In the “repulsive force” case, the metallic film and its scattered field can not be used to guide the atoms through the central slit and deposit them on a semiconductor substrate.

Acknowledgements

This work was performed by the financial support of the Project POSDRU/89/1.5/S/49944

References

- [1] C. Cohen, – Tannoudji, Atomic Motion in Laser Light, J. Dalibard, J. M. Raimond, J. Zinn-Justin, eds., Les Houches, Session LIII, (1990).
- [2] C. Cohen – Tannoudji, J. Dupont-Roc, G. Grynberg, Processus d’interaction entre photons et atomes, InterEditions et Editions du CNRS, Paris, (1988).
- [3] J. Weiner, Light - Matter Interaction, Volume 1 (Fundamentals and Applications), John Wiley & Sons, Inc., Hoboken, New Jersey, (2003).
- [4] G. Leveque, Etude de diffraction d’atomes froids par champs optiques confines, DEA de physique de la Matière – Université Paul Sabatier Toulouse, Juin (2000).
- [5] G. Leveque, C. Meier, R. Mathevet, C. Robilliard, J. Weiner, Physical Review A, Vol. 65, (2002).
- [6] F. J. Garcia - Vidal, L. Martin – Moreno, H. J. Lezec, T. W. Ebbesen, Applied Physics Letters **83**, 22, (2003).
- [7] Harold J. Metcalf and Peter van der Straten „Laser Cooling and Trapping”, Springer - Verlag New York, Inc., (1999).
- [8] J. Moore, R. Pizer, Moment Methods in Electromagnetics, Chichester, England: Research Studies Press, (1984)
- [9] M. A. Morgan., Finite element and Finite Difference Methods in Electromagnetic Scattering, New York: Elsevier, (1990).
- [10] S. B. Balmuş, R. Mathevet J. Weiner, Atom manipulation with micro- and nano-structures emitted light fields, (Poster at FastNet Conference, Les Houches, France, May 2004).
- [11] S. B. Balmuş, Diffraction of the high frequency electromagnetic waves on metallic and dielectric obstacles. Measurement of the dielectric permittivity by the resonant cavity method”, PhD thesis, in romanian, “Al. I. Cuza” University, Iasi, Romania. (July 2007)
- [12] S. B. Balmus, D. D. Sandu, G. O. Avadanei, G. N. Pascariu, Manipulation, J. Optoelectron. Adv. Mater. **11**(6), 782 (2009).
- [13] G. Lévêque, R. Mathevet, C. Girard, B. Viaris, G. Gay, O. Alloschery, S. B. Balmuş, C. O’Dwyer, A. Balocchi, J. Weiner, Coupled resonant rings, (Poster at FastNet Conference, Les Houches, France, May 2004).

*Corresponding author: sorin.balmus@uaic.ro